



Localized solutions for a nonlocal discrete NLS equation



Roberto I. Ben^a, Luís Cisneros Ake^b, A.A. Minzoni^c, Panayotis Panayotaros^{c,*}

^a Instituto de Desarrollo Humano, Universidad Nacional de General Sarmiento, J.M. Gutiérrez 1150, 1613 Los Polvorines, Argentina

^b Department of Mathematics, ESFM, Instituto Politécnico Nacional, Unidad Profesional Adolfo López Mateos Edificio 9, 07738 México D.F., Mexico

^c Depto. Matemáticas y Mecánica, I.I.M.A.S.-U.N.A.M., Apdo. Postal 20-726, 01000 México D.F., Mexico

ARTICLE INFO

Article history:

Received 11 December 2014

Received in revised form 9 March 2015

Accepted 4 April 2015

Available online 14 April 2015

Communicated by C.R. Doering

ABSTRACT

We study spatially localized time-periodic solutions of breather type for a cubic discrete NLS equation with a nonlocal nonlinearity that models light propagation in a liquid crystal waveguide array. We show the existence of breather solutions in the limit where both linear and nonlinear intersite couplings vanish, and in the limit where the linear coupling vanishes with arbitrary nonlinear intersite coupling. Breathers of this nonlocal regime exhibit some interesting features that depart from what is seen in the NLS breathers with power nonlinearity. One property we see theoretically is the presence of higher amplitude at interfaces between sites with zero and nonzero amplitude in the vanishing linear coupling limit. A numerical study also suggests the presence of internal modes of orbitally stable localized modes.

© 2015 Elsevier B.V. All rights reserved.

1. Introduction

We study breather solutions of a discrete nonlinear Schrödinger equation with a nonlocal nonlinearity of Hartree type, modeling the propagation of laser beams in a waveguide array built on a nematic liquid crystal substratum. The model was proposed by Fratallocchi and Assanto [4], and was motivated by experimental and theoretical work reported in [5,6], see also [18]. The interaction between electromagnetic waves and the liquid crystal director field gives rise to a nonlocal nonlinearity for the amplitude equation of a modulated plane wave. This nonlocality has important consequences for the propagation of beams in a bulk (3-D) nematic liquid crystal, as it can stabilize optical solitons propagating through a liquid crystal sample with an appropriate pre-tilt [2, 10,12,15]. Related experimental and theoretical work is reviewed in [14]. The present work suggests some other new effects introduced by the nonlocal nonlinearity in a periodic, waveguide array geometry for the pre-tilted nematic liquid crystal sample.

The first part of the paper concerns the existence of spatially localized solutions of breather type. We present two types of results. First we consider the existence of breather solutions in an analogue of the well-known anticontinuous limit of the cubic NLS equation [9,13,16]. In the present case this limit applies to the vanishing of two parameters, a linear coupling parameter and a nonlocality parameter that is specific to the Hartree-type nonlinearity of the nonlocal DNLS model of [4]. The limiting breathers are identi-

cal to the anticontinuous limit breathers of the cubic DNLS model, and we show that a similar continuation result is applicable to the present case as well. The second result concerns solutions obtained in the limit where only the linear coupling vanishes. The resulting system has a nonlocal nonlinear coupling between the sites, but we can still find breather solutions. These solutions can be in some cases found explicitly, and have slightly different profiles than the ones obtained in the anticontinuous limit of the cubic NLS. An interesting feature of these solutions is that the amplitude is larger at interfaces between sites with zero and nonzero amplitude in the vanishing linear coupling limit. The continuation result is shown for the simplest case where the nonvanishing amplitudes occur at consecutive sites and have the same sign. The presence of interfaces in more general cases is confirmed numerically.

Despite these differences with the cubic NLS, we see that for moderate values of the linear coupling parameter, the nonlocal solutions remain well localized near the sites where the amplitude does not vanish in the uncoupled case. On the other hand, the linear stability analysis shows the possibility of more internal modes. We show that the one-peak breather, which, as in the cubic NLS case is orbitally stable, has internal modes (see [16,17] for the absence of internal modes in the cubic DNLS). The number of internal modes appears to vary with the nonlocality parameter in the nonlinear term. Also, the internal modes have maxima at different distances from the peak of the breather. We see that as the point eigenvalues get closer to the expected continuous spectrum, the maxima of the corresponding internal modes move further away from the peak.

The paper is organized as follows. In Section 2 we state and prove results on the existence of breather solutions. In Section 3

* Corresponding author.

E-mail address: panos@myim.iimas.unam.mx (P. Panayotaros).

we study numerically some breather solutions and their linear stability.

2. Nonlocal discrete NLS equation and breather solutions

We consider the one-dimensional discrete NLS equation

$$\dot{u}_n = \delta i(u_{n+1} + u_{n-1} - 2u_n) + 2\gamma \tanh \frac{\kappa}{2} i \left(\sum_{m \in \mathbb{Z}} e^{-\kappa|m-n|} |u_m|^2 \right) u_n$$

$$n \in \mathbb{Z}, \tag{2.1}$$

with δ, γ, κ real constants, $\kappa > 0$. The model was proposed by Fratallocchi and Assanto [4].

Eq. (2.1) is formally the Hamiltonian system

$$\dot{u}_n = -i \frac{\partial H}{\partial u_n^*}, \quad n \in \mathbb{Z}, \quad \text{with} \tag{2.2}$$

$$H = \delta \sum_{n \in \mathbb{Z}} |u_{n+1} - u_n|^2 - \gamma \tanh \frac{\kappa}{2} \sum_{n \in \mathbb{Z}} \sum_{m \in \mathbb{Z}} |u_m|^2 e^{-\kappa|m-n|} |u_n|^2. \tag{2.3}$$

The quantity $P = \sum_{n \in \mathbb{Z}} |u_n|^2$, also denoted as the *power*, is a conserved quantity.

We consider solutions of (2.1) of the breather form $u_n = e^{-i\omega t} A_n$, with ω real, and $A : \mathbb{Z} \rightarrow \mathbb{C}$ independent of t . Such A satisfies

$$-\omega A_n = \delta(A_{n+1} + A_{n-1} - 2A_n) + 2\gamma \tanh \frac{\kappa}{2} \left(\sum_{m \in \mathbb{Z}} e^{-\kappa|m-n|} |A_m|^2 \right) A_n, \quad \forall n \in \mathbb{Z}. \tag{2.4}$$

In Theorem 2.1 below we show the existence of real solutions in the “anticontinuous”, and local limit, that is for $|\delta|$ small, and κ large respectively. The limit $\kappa \rightarrow \infty, \delta = 0$ breathers are identical to the anticontinuous $\delta = 0$ breathers of the cubic DNLS equation examined by [9] and other authors. The second existence result, Theorem 2.4, concerns continuation from solutions of the $\delta = 0$ problem, i.e. with κ fixed but otherwise arbitrary. The continuation argument is only presented for some special cases. Even these cases reveal some interesting departures from the properties of the power nonlinearity breathers.

Let $X = l_2(\mathbb{Z}, \mathbb{R})$, i.e. the set of real-valued configurations f on \mathbb{Z} , with the norm $\|f\| = (\sum_{n \in \mathbb{Z}} |f_n|^2)^{1/2}$. Let $\{\hat{e}_n\}_{n \in \mathbb{Z}}$ be the standard basis in X .

For $A \in X, \omega \in \mathbb{R}$, and δ, μ real, with $\mu \neq 0$, define $F_n, n \in \mathbb{Z}$, by

$$F_n = \delta(A_{n+1} + A_{n-1} - 2A_n) + 2\gamma \tanh \frac{\kappa}{2} \left(\sum_{m \in \mathbb{Z}} e^{-\kappa|m-n|} A_m^2 \right) A_n + \omega A_n, \tag{2.5}$$

where $\kappa = \mu^{-2}$.

For $A \in X, \omega \in \mathbb{R}$, and $\delta = \mu = 0$, define $F_n, n \in \mathbb{Z}$, by

$$F_n = 2\gamma A_n^3 + \omega A_n. \tag{2.6}$$

Also, for $c > 0, \delta, \mu$ real, and $A \in X, \omega \in \mathbb{R}$, define F_+ by

$$F_+ = \sum_{n \in \mathbb{Z}} A_n^2 - c. \tag{2.7}$$

Let $\mathbf{X} = X \times \mathbb{R}$ with the norm $\|(a, b)\|_{\mathbf{X}} = (\|a\|^2 + |b|^2)^{1/2}$, and let $\mathbf{Y} = \mathbb{R}^2$ with the Euclidean norm. \mathbf{X}, \mathbf{Y} are real Banach spaces. Let $B_{\mathbf{Z}}(\mathbf{z}, r)$ denote the ball of radius r around the point \mathbf{z} of a Banach space \mathbf{Z} . We check that $F = (\{F_n\}_{n \in \mathbb{Z}}(A, \omega, \delta, \mu), F_+(A, \omega, \delta, \mu))$, with F_n, F_+ as in (2.5)–(2.7), defines a function $F : \mathbf{X} \times \mathbf{Y} \rightarrow \mathbf{X}$.

The dependence of F on c is not made explicit in this notation, and the results below are valid for all $c > 0$.

Fix $c > 0$ and consider a nontrivial solution $(A, \omega) = (\tilde{A}, \tilde{\omega})$ of $F(A, \omega, 0, 0) = 0$. By (2.6), (2.7), and $A \in X$, such a solution is determined by two finite disjoint subsets S_+, S_- of \mathbb{Z} , and has the form

$$\tilde{\omega} = -2\gamma\alpha^2, \quad \tilde{A}_n = \pm\alpha, \quad n \in S_{\pm}; \quad \tilde{A}_n = 0, \tag{2.8}$$

$$n \notin S_+ \cup S_-,$$

where α is defined through $(|S_+| + |S_-|)\alpha^2 = c$. We also let $S_0 = \mathbb{Z} \setminus (S_+ \cup S_-)$.

Theorem 2.1. Fix $c > 0$ and consider a nontrivial solution $(A, \omega) = (\tilde{A}, \tilde{\omega})$ of $F(A, \omega, 0, 0) = 0$, as in (2.8). Then there exists $\epsilon_0 > 0$, and a unique continuous two-parameter family $(A, \omega) : B_{\mathbf{Y}}(0, \epsilon_0) \rightarrow \mathbf{X}$, satisfying $(A(0, 0), \omega(0, 0)) = (\tilde{A}, \tilde{\omega})$, and $F(A(\delta, \mu), \omega(\delta, \mu), \delta, \mu) = 0, \forall (\delta, \mu) \in B_{\mathbf{Y}}(0, \epsilon_0)$.

Remark 2.2. The fact that (2.5) involves $\kappa = \mu^{-2}$, and the uniqueness of the continued branch imply that solutions $(A(\delta, -\mu), \omega(\delta, -\mu)), (A(\delta, \mu), \omega(\delta, \mu))$ of (2.4) coincide. The definition $\kappa = \mu^{-2}$ keeps the exponent of $e^{-\kappa|l|}$ in (2.5) negative in the vicinity of $\mu = 0$, unlike e.g. the choice $\kappa = \mu^{-1}$. This allows us to apply a standard continuation statement directly, see the proof below.

Proof. We will apply the Implicit Function Theorem around a solution $(\mathbf{x}, \mathbf{y}) = (\mathbf{x}_0, \mathbf{y}_0)$ of $F = 0$, where $\mathbf{x}_0 = (\tilde{A}, \tilde{\omega}), \tilde{A}, \tilde{\omega}$ as in (2.8), and $\mathbf{y}_0 = (0, 0)$ of $F = 0$. We must check that the (Fréchet) derivative (i) $D_1 F(\mathbf{x}_0, \mathbf{y}_0)$ exists and is a linear isomorphism of \mathbf{X} , and that (ii) F and $D_1 F$ are both continuous at $(\mathbf{x}_0, \mathbf{y}_0)$, see e.g. [20].

We compute $D_1 F$ at $(\mathbf{x}_0, \mathbf{y}_0)$ using (2.6) and taking partial derivatives of $F_n, n \in \mathbb{Z}, F_+$ with respect to $A_n, n \in \mathbb{Z}, \omega$,

$$\frac{\partial F_n}{\partial A_n} = \tilde{\omega} + 6\gamma\tilde{A}_n^2, \quad \frac{\partial F_n}{\partial A_l} = 0, \quad \forall n \in \mathbb{Z}, \quad l \in \mathbb{Z} \setminus \{n\}, \tag{2.9}$$

$$\frac{\partial F_n}{\partial \omega} = \tilde{A}_n, \quad \frac{\partial F_+}{\partial A_n} = 2\tilde{A}_n, \quad \forall n \in \mathbb{Z}, \quad \frac{\partial F_+}{\partial \omega} = 0. \tag{2.10}$$

It is easy to check that the resulting infinite matrix of partial derivatives is the derivative $D_1 F$ at $(\mathbf{x}_0, \mathbf{y}_0)$, we omit the details.

To check invertibility of $D_1 F$ at $(\mathbf{x}_0, \mathbf{y}_0)$, we enumerate the entries of $D_1 F$ as follows. The components of F are ordered as $F_{v_{\pm}(j)}, j \in S_{\pm}, F_{v_0(j)}, j \in S_0$, where the v_{\pm}, v_0 enumerate the elements of S_{\pm}, S_0 respectively. The variables are ordered as $A_{v_{\pm}(j)}, j \in S_{\pm}, A_{v_0(j)}, j \in S_0$. Then $D_1 F(\tilde{A}, \tilde{\omega}, 0, 0)$ has the block diagonal form

$$D_1 F(\tilde{A}, \tilde{\omega}, 0, 0) = \begin{bmatrix} M_1 & 0 \\ 0 & M_2 \end{bmatrix}, \tag{2.11}$$

where M_1 is $(m + 1) \times (m + 1)$, $m = |S_+| + |S_-|$, and $M_2 = -2\gamma\alpha^2 \tilde{I}_0$, with \tilde{I}_0 the identity in \tilde{X}_0 , the span of the $\hat{e}_n, n \in S_0$. To show that $D_1 F(\tilde{A}, \tilde{\omega}, 0, 0)$ is invertible it is enough to check that M_1 is nonsingular. The matrix M_1 has the block form

$$M_1 = \begin{bmatrix} A_{\pm} & C \\ 2C^T & 0 \end{bmatrix}, \tag{2.12}$$

where $A_{\pm} = 4\gamma\alpha^2 I_m, I_m$ is the $m \times m$ identity, $C = [C_1, \dots, C_m]^T$, with $C_j = \alpha$, if $j = 1, \dots, |S_+|, C_j = -\alpha$, if $j = |S_+| + 1, \dots, |S_+| + |S_-|$. Applying the LU algorithm we can then bring M_1 to the upper triangular form

$$U = \begin{bmatrix} A_{\pm} & \tilde{c} \\ 0 & \rho \end{bmatrix}, \tag{2.13}$$

with $\rho = 1/2(|S_+| + |S_-|) \neq 0$, thus M_1 is nonsingular.

The continuity of F at $(\mathbf{x}_0, \mathbf{y}_0)$ is checked in Lemma 2.6.

To show the continuity of D_1F at $(\mathbf{x}_0, \mathbf{y}_0)$ we will be using the fact that for $\mathbf{y} \neq \mathbf{y}_0$, (2.5) yields

$$\begin{aligned} \frac{\partial F_n}{\partial A_n} &= -2\delta + \omega + 2\gamma \tanh \frac{\kappa}{2} \left(\sum_{m \in \mathbb{Z}} e^{-\kappa|m-n|} A_m^2 + 2A_n^2 \right), \quad \forall n \in \mathbb{Z}, \\ \frac{\partial F_n}{\partial A_l} &= \delta + 4\gamma \tanh \frac{\kappa}{2} e^{-\kappa|l-n|} A_l A_n, \quad \forall n \in \mathbb{Z}, \quad l \in \{n-1, n+1\}, \\ \frac{\partial F_n}{\partial A_l} &= 4\gamma \tanh \frac{\kappa}{2} e^{-\kappa|l-n|} A_l A_n, \quad \forall n \in \mathbb{Z}, \\ & \quad l \in \mathbb{Z} \setminus \{n-1, n, n+1\}, \end{aligned} \tag{2.14}$$

$$\frac{\partial F_n}{\partial \omega} = A_n, \quad \frac{\partial F_+}{\partial A_n} = 2A_n, \quad \forall n \in \mathbb{Z}, \quad \frac{\partial F_+}{\partial \omega} = 0. \tag{2.15}$$

We check that the resulting infinite matrix of partial derivatives is indeed the derivative D_1F . The continuity of D_1F at $(\mathbf{x}_0, \mathbf{y}_0)$ is shown in Lemma 2.7 below. \square

We now consider real solutions of (2.4) with $\delta = 0$, and fixed $\kappa > 0$. Fix $c > 0$ and consider a nontrivial solution (A, ω) of $F = 0$, with F as in (2.5). We look for solutions $A \in X$, with $A_n \neq 0$ for $n \in S_A$, S_A is a finite set, and $A_n = 0, \forall n \in S_0 = \mathbb{Z} \setminus S_A$. Then $F = 0$, F as in (2.5), becomes

$$-2\gamma \tanh \frac{\kappa}{2} \left(\sum_{m \in S_A} e^{-\kappa|m-n|} A_m^2 \right) = \omega, \quad \forall n \in S_A. \tag{2.16}$$

This is a linear equation for the components $J_m = A_m^2, m \in S_A$, of the vector J , and we also write it as

$$\mathcal{M}J = (-2\gamma \tanh \frac{\kappa}{2})^{-1} \omega \mathcal{E}, \tag{2.17}$$

with $\mathcal{E} = [1, \dots, 1]^T \in \mathbb{R}^{|S_A|}$. \mathcal{M} is defined implicitly by (2.16), (2.17), and we see that it is symmetric and that all its entries are positive. By (2.16) we see that ω and γ must have opposite signs.

If \mathcal{M} is nonsingular, and $\mathcal{M}^{-1}\mathcal{E}$ is positive, then the solutions of $F = 0, F_+ = 0, F, F_+$ as in (2.5), (2.7) are of the form $(A, \omega) = (\tilde{A}, \tilde{\omega})$, with

$$\begin{aligned} \tilde{\omega} &= -2\gamma \tanh \frac{\kappa}{2} c \left[\sum_{m \in S_A} (\mathcal{M}^{-1}\mathcal{E})_m \right]^{-1}, \quad \tilde{A}_n = \pm \sqrt{\tilde{J}_n}, \quad n \in S_{\pm}, \\ \tilde{A}_n &= 0, \quad n \in S_0, \end{aligned} \tag{2.18}$$

where

$$\tilde{J} = c \left[\sum_{m \in S_A} (\mathcal{M}^{-1}\mathcal{E})_m \right]^{-1} \mathcal{M}^{-1}\mathcal{E}, \tag{2.19}$$

and S_+, S_- are disjoint subsets of S_A satisfying $S_A = S_+ \cup S_-$.

Note that (2.17) can have solutions even in the case where \mathcal{M} is singular. It appears however that \mathcal{M} is nonsingular for all choices of the finite set S_A .

An example is given by the choice $S_A = \{n_0, n_0 + 1, \dots, n_0 + m\}$, i.e. $m + 1$ consecutive sites. Then \mathcal{M} is a symmetric $(m + 1) \times (m + 1)$ Toeplitz matrix with first row $[1, \rho, \rho^2, \dots, \rho^m]$, $\rho = e^{-\kappa}$. For $m = 0, 1$, the invertibility of \mathcal{M} is immediate. For $m \geq 2$, \mathcal{M}^{-1} is a symmetric tridiagonal matrix with

$$\begin{aligned} \text{diag}(\mathcal{M}^{-1}) &= ((1 - \rho^2)^{-1}, (1 - \rho^2)^{-1}(1 + \rho^2), \\ & \quad \dots, (1 - \rho^2)^{-1}(1 + \rho^2), (1 - \rho^2)^{-1}), \end{aligned} \tag{2.20}$$

and

$$(\mathcal{M}^{-1})_{k,k+1} = -(1 - \rho^2)^{-1} \rho, \quad \forall k = 1, \dots, m. \tag{2.21}$$

Then

$$\mathcal{M}^{-1}\mathcal{E} = \frac{1}{1 + \rho} [1, 1 - \rho, \dots, 1 - \rho, 1]^T. \tag{2.22}$$

By (2.18), (2.22)

$$\tilde{\omega} = -2\gamma \tanh \frac{\kappa}{2} \frac{c}{1 + \rho} [m(1 - \rho) + 1 + \rho]. \tag{2.23}$$

Remark 2.3. By (2.18), (2.19) the vector $\mathcal{M}^{-1}\mathcal{E}$ is, up to scalars, the amplitude profile at the sites $n_0, \dots, n_0 + m$. Since $1 - \rho < 1$, the amplitude is larger at the two endpoints of n_0 and $n_0 + m$ of S_A (for $m \geq 2$). All other sites have the same amplitude.

We now formulate a continuation statement for the above $\delta = 0$ breathers. The notation is similar to that of Theorem 2.1. Let $c > 0$, and fix $\kappa \neq 0$ and μ satisfying $\mu^{-2} = \kappa$. For $A \in X, \omega \in \mathbb{R}$, and δ real, let

$$\begin{aligned} G_n(A, \omega, \delta) &= F_n(A, \omega, \delta, \mu), \quad n \in \mathbb{Z}; \\ G_+(A, \omega, \delta) &= F_+(A, \omega, \delta, \mu) \end{aligned} \tag{2.24}$$

with F_n, F_+ as in (2.5), (2.7).

Let $\mathbf{X} = X \times \mathbb{R}$ with the norm $\|(a, b)\|_{\mathbf{X}} = (\|a\|^2 + |b|^2)^{1/2}$, and let $\mathbf{Y} = \mathbb{R}$ with the Euclidean norm. \mathbf{X}, \mathbf{Y} are real Banach spaces. Let $B_{\mathbf{Z}}(z, r)$ denote the ball of radius r around the point z of a Banach space \mathbf{Z} . We check that $G = (\{G_n\}_{n \in \mathbb{Z}}(A, \omega, \delta), G_+(A, \omega, \delta))$, with G_n, G_+ as in (2.24), defines a function $G : \mathbf{X} \times \mathbf{Y} \rightarrow \mathbf{X}$. The dependence of G on c, κ is not made explicit in the above notation, and the results below are valid for all $c, \kappa > 0$ (unless otherwise specified).

Theorem 2.4. Fix $c > 0$, and $\kappa > 0$. Let m be a positive integer, and consider a nontrivial solution $(A, \omega) = (\tilde{A}, \tilde{\omega})$ of $G(A, \omega, 0) = 0$ as in (2.18), (2.19), with $S_A = \{n_0, n_0 + 1, \dots, n_0 + m\}$. Then there exists $\delta_0 > 0$, and a unique continuous one-parameter family $(A, \omega) : B_{\mathbf{Y}}(0, \delta_0) \rightarrow \mathbf{X}$, satisfying $(A(0), \omega(0)) = (\tilde{A}, \tilde{\omega})$, and $G(A(\delta), \omega(\delta), \delta) = 0, \forall \delta \in B_{\mathbf{Y}}(0, \delta_0)$.

Proof. We will apply the Implicit Function Theorem around a solution $(\mathbf{x}, \mathbf{y}) = (\mathbf{x}_0, \mathbf{y}_0)$ of $G = 0$, where $\mathbf{x}_0 = (\tilde{A}, \tilde{\omega}), \tilde{A}, \tilde{\omega}$ as in (2.18), (2.19), and $\mathbf{y}_0 = 0$ of $G = 0$. We must check that the (Fréchet) derivative (i) $D_1G(\mathbf{x}_0, \mathbf{y}_0)$ exists and is a linear isomorphism of \mathbf{X} , and that (ii) G and D_1G are both continuous at $(\mathbf{x}_0, \mathbf{y}_0)$, see e.g. [20].

To check invertibility of D_1G at $(\mathbf{x}_0, \mathbf{y}_0)$, we enumerate the entries of D_1G as follows. The components of G are ordered as $G_{\nu_A(j)}, j \in S_A, G_+, G_{\nu_0(j)}, j \in S_0$, where the ν_A, ν_0 enumerate the elements of S_A, S_0 respectively, and $\nu_A(j) = j - n_0 + 1, j = 1, \dots, m + 1$. The variables are ordered as $A_{\nu_A(j)}, j \in S_A, \omega, A_{\nu_0(j)}, j \in S_0$.

By (2.14), (2.15) and (2.18), (2.19) the matrix of partial derivatives (checked to be the derivative) $D_1G(\tilde{A}, \tilde{\omega}, 0)$ has the block diagonal form

$$D_1G(\tilde{A}, \tilde{\omega}, 0) = \begin{bmatrix} M_1 & 0 \\ 0 & M_2 \end{bmatrix}, \tag{2.25}$$

where M_1 is $(m + 2) \times (m + 2)$, $|S_A| = m + 1$, and M_2 is diagonal, with entries

$$\begin{aligned} M_2(n, n) &= \frac{\partial G_n}{\partial A_n}(\tilde{A}, \tilde{\omega}, 0) \\ &= \begin{cases} \tilde{\omega}(1 - e^{\kappa|n-n_0|}), & \text{if } n < n_0 \\ \tilde{\omega}(1 - e^{\kappa|n-(n_0+m)|}), & \text{if } n > n_0 + m. \end{cases} \end{aligned} \tag{2.26}$$

M_2 is then an isomorphism in \tilde{X}_0 , the span of the $\tilde{e}_n, n \in S_0$, to show that $D_1G(\tilde{A}, \tilde{\omega}, 0)$ is invertible it is enough to check that M_1 is nonsingular.

The matrix M_1 has the form

$$M_1 = \begin{bmatrix} M_{+,+} & C \\ 2C^T & 0 \end{bmatrix}, \tag{2.27}$$

where $C = [C_1, \dots, C_{m+1}]^T$, with $C_j = \tilde{A}_{n_0+j-1}$, \tilde{A}_j as in (2.18). Furthermore

$$M_{+,+} = 4\gamma \tanh \frac{\kappa}{2} c \left[\sum_{m \in S_A} (\mathcal{M}^{-1} \mathcal{E})_m \right]^{-1} \frac{1-\rho}{1+\rho} \tilde{M}, \quad \rho = e^{-\kappa}, \tag{2.28}$$

where \tilde{M} is an $(m+1) \times (m+1)$ symmetric matrix. For $m \geq 3$, \tilde{M} has the following structure: The first row r_1 of \tilde{M} is

$$r_1 = \left[\frac{1}{1-\rho}, \frac{\rho}{\sqrt{1-\rho}}, \frac{\rho^2}{\sqrt{1-\rho}}, \dots, \frac{\rho^{m-1}}{\sqrt{1-\rho}}, \frac{\rho^m}{1-\rho} \right], \tag{2.29}$$

and the $m+1$ -th column C_{m+1} of \tilde{M} is

$$C_{m+1} = \left[\frac{\rho^m}{1-\rho}, \frac{\rho^{m-1}}{\sqrt{1-\rho}}, \dots, \frac{\rho}{\sqrt{1-\rho}}, \frac{1}{1-\rho} \right]^T. \tag{2.30}$$

By symmetry r_1 , and C_{m+1} also define the first column C_1 , and $m+1$ -th row r_{m+1} of \tilde{M} respectively. The remaining entries $\tilde{M}_{i,j}$ with $i, j \in \{2, \dots, m\}$ form a symmetric $(m-1) \times (m-1)$ Toeplitz matrix with first row \tilde{r} given by

$$\tilde{r} = [1, \rho, \rho^2, \dots, \rho^{m-2}]. \tag{2.31}$$

The cases $m = 1, 2$ are treated separately, and $M_{+,+}$ is easily seen to be invertible.

For $m \geq 3$ \tilde{M} has a symmetric tridiagonal inverse \tilde{M}^{-1} with diagonal entries

$$\text{diag } \tilde{M}^{-1} = \frac{1}{1-\rho^2} [1-\rho, 1+\rho^2, 1+\rho^2, \dots, 1+\rho^2, 1-\rho], \tag{2.32}$$

and off-diagonal entries

$$\tilde{M}^{-1}(1, 2) = \tilde{M}^{-1}(m, m+1) = -\frac{\rho}{1-\rho^2} \sqrt{1-\rho}, \tag{2.33}$$

$$\tilde{M}^{-1}(j, j+1) = -\frac{\rho}{1-\rho^2}, \quad j = 2, \dots, m-1. \tag{2.34}$$

By (2.28) the matrix $M_{+,+}$ is therefore invertible. To check that M_1 is invertible we use the fact that by (2.27),

$$\det(M_1) = (-2C^T M_{+,+}^{-1} C) \det(M_{+,+}), \tag{2.35}$$

see e.g. [1]. Using the expressions for $M_{+,+}^{-1}$, C above, we compute

$$-2C^T M_{+,+}^{-1} C = -\frac{2+(m-1)(1-\rho)}{2\gamma(1+\rho) \tanh \frac{\kappa}{2}}, \tag{2.36}$$

which does not vanish. This concludes the proof of invertibility of D_1G at $(\mathbf{x}_0, \mathbf{y}_0)$. The continuity of G and D_1G at $(\mathbf{x}_0, \mathbf{y}_0)$ is shown in Lemmas 2.8, 2.9 respectively. \square

Remark 2.5. We can obtain analogous continuation results with ω fixed, e.g. as in [13]. We expect the proofs to be similar. The present version is more natural for studies of the dynamics of the lattice in the reduced phase space, obtained first by fixing P , see e.g. [11] for a finite lattice. The continuation arguments also apply to finite lattices since the blocks corresponding to S_+ , S_0 in D_1F , and D_1G are the same.

We now show the continuity of the functions F, G and their derivatives at the continued solutions.

Lemma 2.6. Fix $c > 0$ and consider the solution $(\mathbf{x}, \mathbf{y}) = (\mathbf{x}_0, \mathbf{y}_0)$ of $F = 0$, with $\mathbf{x}_0 = (\tilde{A}, \tilde{\omega})$, $\mathbf{y}_0 = (\delta, \mu) = (0, 0)$, as in (2.8). Then F is continuous at $(\mathbf{x}_0, \mathbf{y}_0)$.

Proof. To check the continuity of F at $(\mathbf{x}_0, \mathbf{y}_0)$ we examine $\|F(\mathbf{x}, \mathbf{y}) - F(\mathbf{x}_0, \mathbf{y}_0)\|$ as $(\mathbf{x}, \mathbf{y}) = (A, \omega, \delta, \mu)$ approaches $(\mathbf{x}_0, \mathbf{y}_0)$ in $\mathbf{X} \times \mathbf{Y}$. $F(\mathbf{x}_0, \mathbf{y}_0)$ is evaluated using (2.6), (2.7). $F(\mathbf{x}, \mathbf{y})$ is evaluated using (2.5), (2.7), if $\mathbf{y} \neq \mathbf{y}_0$, and (2.6) otherwise. We have

$$F_+(\mathbf{x}, \mathbf{y}) - F_+(\mathbf{x}_0, \mathbf{y}_0) = \|A\|^2 - \|\tilde{A}\|^2 \rightarrow 0 \tag{2.37}$$

as $\|A - \tilde{A}\| \rightarrow 0$. Also, for $\mathbf{y} \neq \mathbf{y}_0$, $n \in \mathbb{Z}$

$$F_n(\mathbf{x}, \mathbf{y}) - F_n(\mathbf{x}_0, \mathbf{y}_0) = \delta(\Delta A)_n + \omega A_n - \tilde{\omega} \tilde{A}_n + 2B_n, \tag{2.38}$$

with

$$B_n = \gamma \tanh \frac{\kappa}{2} \left(\sum_{m \in \mathbb{Z}} e^{-\kappa|m-n|} A_m^2 \right) A_n - \gamma \tilde{A}_n^3. \tag{2.39}$$

Letting $B = \{B_n\}_{n \in \mathbb{Z}}$, we then have

$$\left(\sum_{n \in \mathbb{Z}} |F_n(\mathbf{x}, \mathbf{y}) - F_n(\mathbf{x}_0, \mathbf{y}_0)|^2 \right)^{1/2} \leq |\delta| \|\Delta\|_{X,X} \|A\| + |\omega| \|A - \tilde{A}\| + |\omega - \tilde{\omega}| \|\tilde{A}\| + 2\|B\|. \tag{2.40}$$

The first three terms vanish as $A \rightarrow \tilde{A}$ in X , and $|\delta| \rightarrow 0$, $\omega \rightarrow \tilde{\omega}$. To estimate $\|B\|$, let

$$g_n(A, \mu) = \sum_{m \in \mathbb{Z}} e^{-\kappa|m-n|} A_m^2, \quad n \in \mathbb{Z}, \tag{2.41}$$

and write

$$B = \gamma(K + L + M), \quad \text{with } K_n = \left(\tanh \frac{\kappa}{2} - 1 \right) g_n(A, \mu) A_n, \\ L_n = (g_n(A, \mu) - A_n^2) A_n, \quad M_n = A_n^3 - \tilde{A}_n^3, \quad \forall n \in \mathbb{Z}. \tag{2.42}$$

By (2.41), we have $g_n(A, \mu) \leq \|A\|^2$, $\forall n \in \mathbb{Z}$, hence

$$\|K\|^2 \leq \left| \tanh \frac{\kappa}{2} - 1 \right| \sum_{n \in \mathbb{Z}} |g_n(A, \mu)|^2 A_n^2 \\ \leq \left| \tanh \frac{\kappa}{2} - 1 \right| \|A\|^6. \tag{2.43}$$

Also,

$$\|M\|^2 \leq \sum_{n \in \mathbb{Z}} (A_n^2 + A_n \tilde{A}_n + \tilde{A}_n^2)^2 |A_n - \tilde{A}_n|^2 \\ \leq C(\|A\|, \|\tilde{A}\|) \|A - \tilde{A}\|^2, \tag{2.44}$$

with C a fixed function of $\|A\|, \|\tilde{A}\|$, and

$$\|L\|^2 \leq \sum_{n \in \mathbb{Z}} \left(\sum_{m \in \mathbb{Z} \setminus \{n\}} e^{-\kappa|m-n|} A_m^2 \right)^2 |A_n|^2 \leq e^{-2\kappa} \|A\|^6. \tag{2.45}$$

By (2.43), (2.44), (2.44), and (2.42), $\|B\|$ also vanishes as $\mu \rightarrow 0$ (i.e. $\kappa \rightarrow +\infty$), $A \rightarrow \tilde{A}$ in X , as required. \square

Lemma 2.7. Fix $c > 0$ and consider the solution $(\mathbf{x}, \mathbf{y}) = (\mathbf{x}_0, \mathbf{y}_0)$ of $F = 0$, with $\mathbf{x}_0 = (\tilde{A}, \tilde{\omega})$, $\mathbf{y}_0 = (\delta, \mu) = (0, 0)$, as in (2.8). Then D_1F is continuous at $(\mathbf{x}_0, \mathbf{y}_0)$.

Proof. To show the continuity of D_1F at $(\mathbf{x}_0, \mathbf{y}_0)$, it is enough to show that

$$\| [D_1F(\mathbf{x}, \mathbf{y}) - D_1F(\mathbf{x}_0, \mathbf{y}_0)]v \| \leq \beta \|v\|, \quad \forall v \in \mathbf{X}, \quad (2.46)$$

with β that is independent of v , and satisfies $\beta \rightarrow 0$ as $(\mathbf{x}, \mathbf{y}) \rightarrow (\mathbf{x}_0, \mathbf{y}_0)$ in $\mathbf{X} \times \mathbf{Y}$.

Let $v = (\{v_n\}_{n \in \mathbb{Z}}, v_+)$, $w = (\{w_n\}_{n \in \mathbb{Z}}, w_+)$, where

$$w = Mv, \quad M = [D_1F(\mathbf{x}, \mathbf{y}) - D_1F(\mathbf{x}_0, \mathbf{y}_0)]. \quad (2.47)$$

Then, by (2.9), (2.10), (2.14), (2.15), and $\mathbf{y} \neq \mathbf{y}_0$, $n \in \mathbb{Z}$,

$$\begin{aligned} w_n &= \sum_{m \in \mathbb{Z}} M_{n,m} v_m + M_{n,+} v_+ \\ &= \delta(\Delta v)_n + (\omega - \tilde{\omega})v_n \\ &\quad + 2\gamma \left[\tanh \frac{\kappa}{2} (3A_n^2 + \sum_{m \in \mathbb{Z} \setminus \{n\}} e^{-\kappa|m-n|} A_m^2) - 3\tilde{A}_n^2 \right] v_n \\ &\quad + 4\gamma \tanh \frac{\kappa}{2} \left(\sum_{m \in \mathbb{Z} \setminus \{n\}} e^{-\kappa|m-n|} A_m v_m \right) A_n + 2(A_n - \tilde{A}_n)v_+ \\ &= \delta(\Delta v)_n + (\omega - \tilde{\omega})v_n + 2\gamma (J'_n + K'_n + L'_n) \\ &\quad + 2(A_n - \tilde{A}_n)v_+, \end{aligned} \quad (2.48)$$

where

$$\begin{aligned} J'_n &= (3 \tanh \frac{\kappa}{2} A_n^2 - 3\tilde{A}_n^2)v_n, \\ K'_n &= \tanh \frac{\kappa}{2} \left(\sum_{m \in \mathbb{Z} \setminus \{n\}} e^{-\kappa|m-n|} A_m^2 \right) v_n, \\ L'_n &= 2 \tanh \frac{\kappa}{2} \left(\sum_{m \in \mathbb{Z} \setminus \{n\}} e^{-\kappa|m-n|} A_m v_m \right) A_n, \quad \forall n \in \mathbb{Z}. \end{aligned} \quad (2.49)$$

Then

$$|K'_n| \leq \left| \tanh \frac{\kappa}{2} \right| \|A\|^2 \|v_n\|, \quad \forall n \in \mathbb{Z}, \quad (2.50)$$

therefore

$$\sum_{n \in \mathbb{Z}} |K'_n|^2 \leq \left| \tanh \frac{\kappa}{2} \right|^2 \|A\|^4 \|v\|^2. \quad (2.51)$$

Similarly by (2.49),

$$J'_n = 3 \left[(\tanh \frac{\kappa}{2} - 1) A_n^2 + (A_n^2 - \tilde{A}_n^2) \right] v_n, \quad \forall n \in \mathbb{Z}, \quad (2.52)$$

therefore

$$\begin{aligned} \sum_{n \in \mathbb{Z}} |J'_n|^2 &\leq 18 \left[(\tanh \frac{\kappa}{2} - 1)^2 \sup_{n \in \mathbb{Z}} |A_n|^4 + \sup_{n \in \mathbb{Z}} |\tilde{A}_n^2 - A_n^2|^2 \right] \|v\|^2 \\ &\leq 18 \left[(\tanh \frac{\kappa}{2} - 1)^2 \|A\|^4 \right. \\ &\quad \left. + 2 \|A - \tilde{A}\|^2 (\|A\|^2 + \|\tilde{A}\|^2) \right] \|v\|^2. \end{aligned} \quad (2.53)$$

Also by (2.49),

$$\begin{aligned} \sum_{n \in \mathbb{Z}} |L'_n|^2 &\leq 4 \left| \tanh \frac{\kappa}{2} \right|^2 \sum_{n \in \mathbb{Z}} \left| \sum_{m \in \mathbb{Z} \setminus \{n\}} e^{-\kappa|m-n|} A_m v_m \right|^2 A_n^2 \\ &\leq 4 \left| \tanh \frac{\kappa}{2} \right|^2 \sum_{n \in \mathbb{Z}} \left(\sum_{m \in \mathbb{Z} \setminus \{n\}} e^{-2\kappa|m-n|} A_m^2 \right) \left(\sum_{m \in \mathbb{Z} \setminus \{n\}} v_m^2 \right) A_n^2 \\ &\leq 4 \left| \tanh \frac{\kappa}{2} \right|^2 \sum_{n \in \mathbb{Z}} e^{-2\kappa} \left(\sum_{m \in \mathbb{Z} \setminus \{n\}} A_m^2 \right) \|v\|^2 A_n^2 \\ &\leq 4 \left| \tanh \frac{\kappa}{2} \right|^2 e^{-2\kappa} \|A\|^4 \|v\|^2. \end{aligned} \quad (2.54)$$

Also,

$$w_+ = \sum_{m \in \mathbb{Z}} M_{+,m} v_m + M_{+,+} v_+ = 2 \sum_{m \in \mathbb{Z}} (A_m - \tilde{A}_m) v_m, \quad (2.55)$$

therefore

$$w_+^2 \leq 4 \|A - \tilde{A}\|^2 \|v\|^2. \quad (2.56)$$

Combining (2.48), (2.51), (2.53), (2.54), (2.56),

$$\|w\|_{\mathbf{X}}^2 = \sum_{n \in \mathbb{Z}} |w_n|^2 + |w_+|^2 \leq \beta^2 \|v\|^2, \quad (2.57)$$

where

$$\begin{aligned} \beta^2 &\leq 40 \left[\delta \|\Delta\|_{X,X} + (\omega - \tilde{\omega})^2 + 2 \|A - \tilde{A}\|^2 + \gamma^2 \left| \tanh \frac{\kappa}{2} \right|^2 \|A\|^4 \right. \\ &\quad \left. + 18 \left[\gamma^2 \left(\tanh \frac{\kappa}{2} - 1 \right)^2 \|A\|^4 + 2 \|A - \tilde{A}\|^2 (\|A\|^2 + \|\tilde{A}\|^2) \right] \right. \\ &\quad \left. + 4 \gamma^2 \left| \tanh \frac{\kappa}{2} \right|^2 e^{-2\kappa} \|A\|^4 \right]. \end{aligned} \quad (2.58)$$

Thus $\beta \rightarrow 0$ as $(\mathbf{x}, \mathbf{y}) \rightarrow (\mathbf{x}_0, \mathbf{y}_0)$, as required in (2.46). \square

Lemma 2.8. Fix $c > 0$, and fix $\kappa > 0$. Then $G : \mathbf{X} \times \mathbf{Y} \rightarrow \mathbf{X}$, defined as in (2.24), is continuous in $\mathbf{X} \times \mathbf{Y}$.

Proof. To avoid extra notation we will show the continuity of G at $(\mathbf{x}_0, \mathbf{y}_0) = (\tilde{A}, \tilde{\omega}, 0)$, with $\tilde{A}, \tilde{\omega}$ as in (2.18) with $S_A = \{n_0, n_0 + 1, \dots, n_0 + m\}$, as needed for the implicit function theorem. The proof is applicable to arbitrary $(\mathbf{x}_0, \mathbf{y}_0) \in \mathbf{X} \times \mathbf{Y}$.

We show that $\|G(\mathbf{x}, \mathbf{y}) - G(\mathbf{x}_0, \mathbf{y}_0)\| \rightarrow 0$ as $(\mathbf{x}, \mathbf{y}) = (A, \omega, \delta)$ approaches $(\mathbf{x}_0, \mathbf{y}_0)$ in $\mathbf{X} \times \mathbf{Y}$.

By $G_+ = F_+$, we have $G_+(\mathbf{x}, \mathbf{y}) - G_+(\mathbf{x}_0, \mathbf{y}_0) \rightarrow 0$ as $\|A - \tilde{A}\| \rightarrow 0$, as in (2.37).

By (2.24), (2.5)

$$\begin{aligned} &\left(\sum_{n \in \mathbb{Z}} |G_n(\mathbf{x}, \mathbf{y}) - G_n(\mathbf{x}_0, \mathbf{y}_0)|^2 \right)^{1/2} \\ &\leq |\delta| \|\Delta\|_{X,X} \|A\| + |\omega| \|A - \tilde{A}\| + |\omega - \tilde{\omega}| \|\tilde{A}\| \\ &\quad + 2|\gamma| \tanh \frac{\kappa}{2} \|\tilde{B}\|, \end{aligned} \quad (2.59)$$

with $\tilde{B} = \{\tilde{B}_n\}_{n \in \mathbb{Z}}$,

$$\tilde{B}_n = \gamma \tanh \frac{\kappa}{2} \left(g_n(A) A_n - g_n(\tilde{A}) \tilde{A}_n \right), \quad (2.60)$$

and $g_n(A)$ as in (2.41), $\forall n \in \mathbb{Z}$. The first three terms in (2.59) vanish as $A \rightarrow \tilde{A}$ in X , and $|\delta| \rightarrow 0$, $\omega \rightarrow \tilde{\omega}$. To estimate $\|\tilde{B}\|$ we use

$$\begin{aligned} |\tilde{B}_n| &\leq |g_n(A)| |A_n - \tilde{A}_n| + |g_n(A) - g_n(\tilde{A})| |\tilde{A}_n| \\ &\leq \|A\|^2 |A_n - \tilde{A}_n| + |\tilde{A}_n| \sum_{m \in \mathbb{Z}} |A_m^2 - \tilde{A}_m^2| \\ &\leq \|A\|^2 |A_n - \tilde{A}_n| + |\tilde{A}_n| (\|A\| + \|\tilde{A}\|) \|A - \tilde{A}\|. \end{aligned} \quad (2.61)$$

By (2.60), (2.61) it follows that $\|\tilde{B}\| \rightarrow 0$ as $\|A - \tilde{A}\| \rightarrow 0$, as required. \square

Lemma 2.9. Fix $c, \kappa > 0$ and consider $G : \mathbf{X} \times \mathbf{Y} \rightarrow \mathbf{X}$, defined as in (2.24), Then D_1G is continuous in $\mathbf{X} \times \mathbf{Y}$.

Proof. To avoid extra notation we will show the continuity of D_1G at $(\mathbf{x}_0, \mathbf{y}_0) = (\tilde{A}, \tilde{\omega}, \tilde{\delta})$, with $\tilde{A}, \tilde{\omega}$ as in (2.18) with $S_A = \{n_0, n_0 + 1, \dots, n_0 + m\}$, $\tilde{\delta} = 0$ as needed for the implicit function theorem. The proof is applicable to arbitrary $(\mathbf{x}_0, \mathbf{y}_0) \in \mathbf{X} \times \mathbf{Y}$.

To show the continuity of D_1G at $(\mathbf{x}_0, \mathbf{y}_0)$, it is enough to show that

$$\| [D_1G(\mathbf{x}, \mathbf{y}) - D_1G(\mathbf{x}_0, \mathbf{y}_0)]v \| \leq \beta \|v\|, \quad \forall v \in \mathbf{X}, \quad (2.62)$$

with β that is independent of v , and satisfies $\beta \rightarrow 0$ as $(\mathbf{x}, \mathbf{y}) \rightarrow (\mathbf{x}_0, \mathbf{y}_0)$ in $\mathbf{X} \times \mathbf{Y}$.

Let $v = (\{v_n\}_{n \in \mathbb{Z}}, v_+)$, $w = (\{w_n\}_{n \in \mathbb{Z}}, w_+)$, where

$$w = Mv, \quad M = [D_1G(\mathbf{x}, \mathbf{y}) - D_1G(\mathbf{x}_0, \mathbf{y}_0)]. \quad (2.63)$$

It is clear from the definitions of F , and G , in (2.5), (2.7), and (2.24) respectively that $D_1F(A, \omega, \delta, \mu) = D_1G(A, \omega, \delta)$ for any fixed $\mu^2 = \kappa^{-1}$, i.e. $\mu \neq 0$, and we calculate D_1G using (2.14), (2.15). Then

$$\begin{aligned} w_n &= \sum_{m \in \mathbb{Z}} M_{n,m} v_m + M_{n,+} v_+ \\ &= (\delta - \tilde{\delta})(\Delta v)_n + (\omega - \tilde{\omega})v_n \\ &\quad + 2\gamma [\tanh \frac{\kappa}{2} [(g_n(A) - g_n(\tilde{A})) + 2A_n^2 - 2\tilde{A}_n^2] v_n \\ &\quad + 4\gamma [\tanh \frac{\kappa}{2} \left[\left(\sum_{m \in \mathbb{Z} \setminus \{n\}} A_m v_m \right) A_n - \left(\sum_{m \in \mathbb{Z} \setminus \{n\}} \tilde{A}_m v_m \right) \tilde{A}_n \right] \\ &\quad + 2(A_n - \tilde{A}_n)v_+] \\ &= (\delta - \tilde{\delta})(\Delta v)_n + (\omega - \tilde{\omega})v_n + 2\gamma [\tanh \frac{\kappa}{2} (2\tilde{I}_n + \tilde{K}_n + 2\tilde{L}_n) \\ &\quad + 2(A_n - \tilde{A}_n)v_+], \end{aligned} \quad (2.64)$$

$$\begin{aligned} \tilde{I}_n &= (A_n^2 - \tilde{A}_n^2)v_n, \quad \tilde{K}_n = \left(\sum_{m \in \mathbb{Z}} e^{-\kappa|m-n|} (A_m^2 - \tilde{A}_m^2) \right) v_n, \\ \tilde{L}_n &= \sum_{m \in \mathbb{Z} \setminus \{n\}} (A_m v_m) A_n - \sum_{m \in \mathbb{Z} \setminus \{n\}} (\tilde{A}_m v_m) \tilde{A}_n, \end{aligned} \quad (2.65)$$

$\forall n \in \mathbb{Z}$. Then, arguing as in (2.61)

$$\sum_{n \in \mathbb{Z}} |\tilde{I}_n|^2 \leq 2(\|A\|^2 + \|\tilde{A}\|^2) \|A - \tilde{A}\|^2 \|v\|^2. \quad (2.66)$$

Similarly

$$|\tilde{K}_n| \leq \sum_{m \in \mathbb{Z}} e^{-\kappa|m-n|} |A_m^2 - \tilde{A}_m^2| |v_n|, \quad (2.67)$$

so that arguing again as in (2.61) we have

$$\sum_{n \in \mathbb{Z}} |\tilde{K}_n|^2 \leq 2(\|A\|^2 + \|\tilde{A}\|^2) \|A - \tilde{A}\|^2 \|v\|^2. \quad (2.68)$$

Also,

$$\begin{aligned} |\tilde{L}_n| &\leq \left| \sum_{m \in \mathbb{Z} \setminus \{n\}} (A_m - \tilde{A}_m) v_m \|A_n\| + \left| \sum_{m \in \mathbb{Z} \setminus \{n\}} \tilde{A}_m v_m \|A_n - \tilde{A}_n\| \right| \\ &\leq \|A - \tilde{A}\| \|v\| \|A_n\| + \|\tilde{A}\| \|v\| \|A_n - \tilde{A}_n\|. \end{aligned} \quad (2.69)$$

Therefore

$$\sum_{n \in \mathbb{Z}} |\tilde{L}_n|^2 \leq (\|A\|^2 + \|\tilde{A}\|^2) \|A - \tilde{A}\|^2 \|v\|^2. \quad (2.70)$$

Combining (2.66), (2.68), (2.70),

$$\|w\|_{\mathbf{X}}^2 = \sum_{n \in \mathbb{Z}} |w_n|^2 + |w_+|^2 \leq \tilde{\beta}^2 \|v\|^2, \quad (2.71)$$

where

$$\begin{aligned} \tilde{\beta} &\leq |(\delta - \tilde{\delta}) \|\Delta\|_{X,X} + |\omega - \tilde{\omega}| \\ &\quad + 132(|\gamma| \tanh \frac{\kappa}{2} (\|A\| + \|\tilde{A}\|)^{1/2} + 1) \|A - \tilde{A}\| \end{aligned} \quad (2.72)$$

Thus $\beta \rightarrow 0$ as $(\mathbf{x}, \mathbf{y}) \rightarrow (\mathbf{x}_0, \mathbf{y}_0)$, as required. \square

3. Numerical examples of breathers and their stability

We now examine two types of examples of breathers, one-peak breathers, and shelf-shaped breathers. In the first case we show evidence for the existence of internal modes. In the second case we exhibit the property of amplitude increase at interfaces. Both features are a consequence of the nonlocal nonlinearity.

In what follows we consider (2.1) with $\gamma = -1$. δ negative/positive correspond the “focusing/defocusing” sign combinations respectively.

To study the relative stability of a breather solution we write (2.1) in the variables v defined by $u = e^{-i\omega t} v$. Hamilton’s equation (2.2) then becomes

$$\dot{v}_n = -i \frac{\partial H_\omega}{\partial v_n^*}, \quad n \in \mathcal{I}, \quad \text{with } H_\omega = H - \omega P. \quad (3.1)$$

The index set \mathcal{I} here is \mathbf{Z} . Breather solutions $u = e^{-i\omega t} A$ of (2.1) correspond to fixed points A of (3.1). This also implies that points $e^{i\theta} A$, $\theta \in \mathbf{R}$, are also fixed points of (3.1).

Let $z = [q, p]^T$, with $z_n = [q_n, p_n]^T$, $q_n = \text{Re} v_n$, $p_n = \text{Im} v_n$, $n \in \mathcal{I}$. Then (3.1) is also written as

$$\dot{z} = J \nabla h_\omega, \quad \text{with } h_\omega = \frac{1}{2} H_\omega, \quad (3.2)$$

and $(Jz)_n = -[p_n, q_n]^T$, i.e. J is the standard symplectic operator in X . The linearization at a fixed point A of (3.1) is

$$\dot{z} = J \mathcal{H} z, \quad \text{with } \mathcal{H} = \nabla^2 h_\omega(A), \quad (3.3)$$

i.e. \mathcal{H} is the Hessian of h_ω at A (the dependence of \mathcal{H} on ω is suppressed from the notation).

In the case of real breather $A_n \in \mathbf{R}$, $\forall n \in \mathcal{I}$, (3.3) is equivalent to the quadratic Hamiltonian system

$$\dot{z} = J \nabla h, \quad \text{with } h = \frac{1}{2} \langle p, L_+ p \rangle + \frac{1}{2} \langle q, L_- q \rangle, \quad (3.4)$$

where $\langle \cdot, \cdot \rangle$ the standard inner product in $l^2(\mathbb{Z}; \mathbb{R})$, and L_+ , L_- are linear operators defined as follows. First define the linear operators \mathcal{A} , $\mathcal{M} : X \rightarrow X$ by

$$\mathcal{A}(n, k) = \tanh \frac{\kappa}{2} \left(\sum_{m \in \mathbb{Z}} e^{-\kappa|m-n|} A_m^2 \right) \delta_{n,k}, \quad n, k \in \mathcal{I}, \quad (3.5)$$

$$\mathcal{M}(n, k) = \tanh \frac{\kappa}{2} e^{-\kappa|m-k|} A_k A_n, \quad n, k \in \mathcal{I}, \quad (3.6)$$

with $\delta_{n,k}$ the Kronecker delta. Then

$$L_- = -\omega I - \delta \Delta + 2\mathcal{A}, \quad L_+ = -\omega I - \delta \Delta + 2\mathcal{A} + 4\mathcal{M}. \quad (3.7)$$

In the case where X is $l^2(\mathbf{Z}; \mathbf{C})$, and $A \in X$, the symmetric operators L_+ , L_- are bounded.

Numerical calculations use a finite domain with N sites. The equations are the same, with $\mathcal{I} = \{1, \dots, N\}$, and $X = \mathbf{C}^N$. The definition of Δ at the sites 1, N is as in [11], and is equivalent to imposing the discrete analogue of Dirichlet boundary conditions.

In Figs. 1a, 2a we show two breather solutions with $\kappa = 0.5$, $\kappa = 0.25$ respectively. In both cases $\delta = -0.5$, $\gamma = -1$ (focusing case). Figs. 1b, 2b show the respective spectra of $J\mathcal{H}$. The eigenvalues come in pairs $\pm i\lambda$, λ real, indicating linear stability. The corresponding Hessian \mathcal{H} has one zero eigenvalue, one positive eigenvalue, and all remaining eigenvalues are negative. We also have

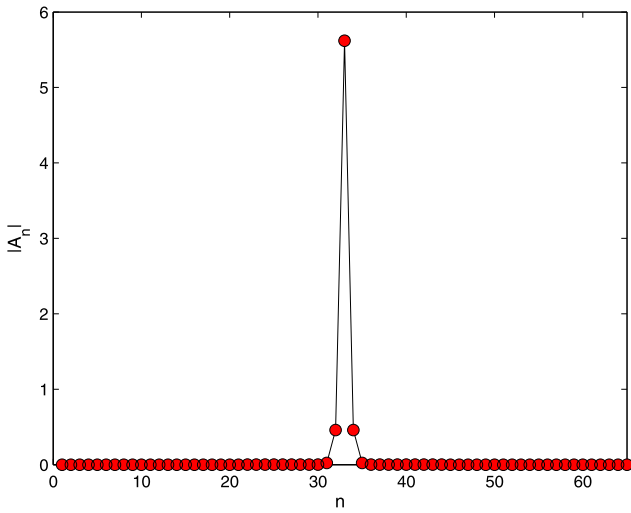


Fig. 1a. $|A_n|$ vs. site number n for a 1-peak breather that is strongly localized at central site $n = 33$. The number of sites is $N = 65$, while $\kappa = 0.5$, $\delta = -0.5$, $\gamma = -1$ (focusing case). The power is $c = 32.0$. The computed frequency is $\omega = 14.6749972$.

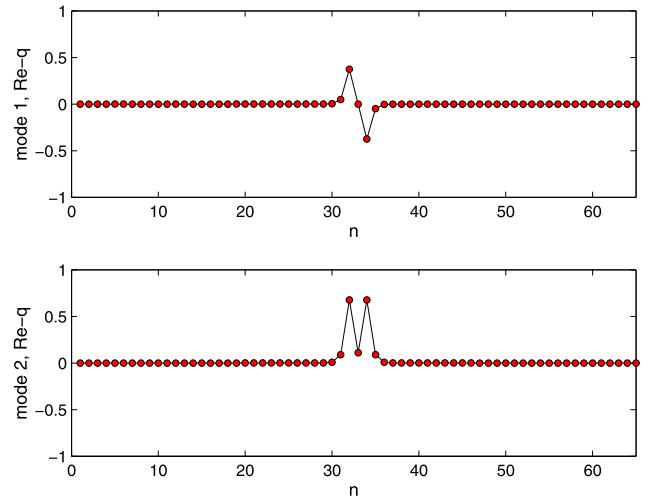


Fig. 1c. q_n vs. n , q -component of real part of eigenvectors of $J\mathcal{H}$ corresponding to eigenvalues $\pm i\lambda_1 = \pm i6.02074736$ (“mode 1”, odd), and $\pm i\lambda_2 = \pm i6.07033363$ (“mode 2”, even) respectively. These are the nonzero eigenvalues that are nearest to the origin.

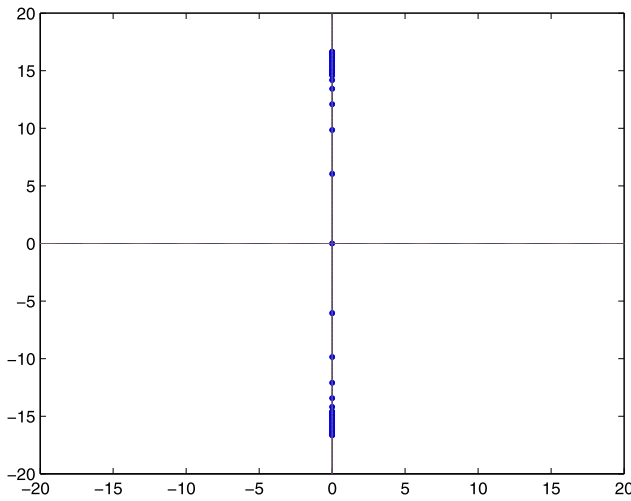


Fig. 1b. Spectrum of $J\mathcal{H}$ around breather of Fig. 1a. Eigenvalues come in pairs $\pm i\lambda$, indicating linear stability. Closer inspection suggests 12 pairs of isolated (point) eigenvalues $\pm i\lambda$, and a remaining set of closely spaced eigenvalues thought to represent continuous spectrum for the infinite problem. The eigenvalues in the continuous band have positive real parts in the interval $[14.6799965, 16.6643367]$.

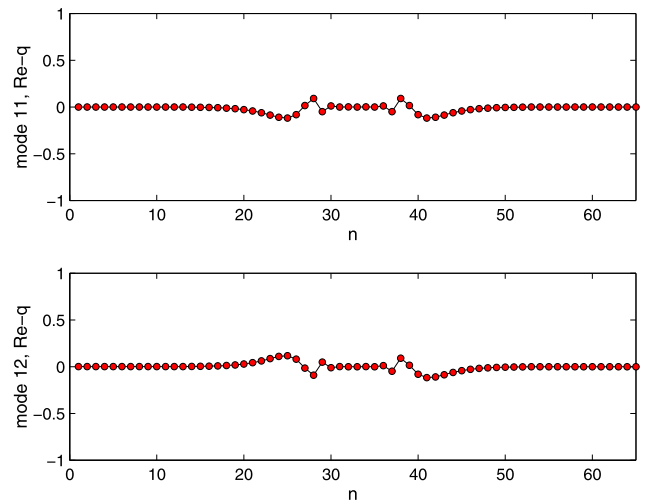


Fig. 1d. q_n vs. n , q -component of real part of eigenvectors of $J\mathcal{H}$ corresponding to eigenvalues $\pm i\lambda_{11} = \pm i14.5734663$ (“mode 11”, even), and $\pm i\lambda_{12} = \pm i14.5734663$ (“mode 12”, odd). These are the highest frequency internal modes.

evidence that $P'(\omega) > 0$, where the derivative is approximated by computing breather solutions with nearby powers. By [7], applied to local maxima (i.e. with signs suitably reversed), these breathers are expected to be local maxima of the Hamiltonian H on the hypersphere $P = c$, and therefore orbitally stable.

The interesting observation is that Figs. 1b, 2b suggest the existence of both discrete and continuous spectrum for $J\mathcal{H}$ of the infinite lattice problem. In the case of the example of Fig. 1, obtained for $N = 65$, closer inspection of the eigenvalues of $J\mathcal{H}$ with positive imaginary part suggests there are 12 eigenvalues $i\lambda_j$ (counted with multiplicity) with $\lambda_j \in [6.02074736, 14.5734663]$, and that the remaining eigenvalues are more densely spaced, and have imaginary part contained in the interval $[14.6752636, 16.674649]$. The distinction between the first 12 eigenvalues and the remaining ones is becoming clearer as we increase the number of sites, e.g. from $N = 65$ up to $N = 523$. We obtain the same breather solution A_n (in the common lattice points, up to double precision) and frequency ω , and the same 12 eigenvalues $i\lambda_j$ (counted with multiplicity) in the interval $\lambda_j \in [6.02074736, 14.5734663]$, while the remaining eigenvalues become denser in an interval

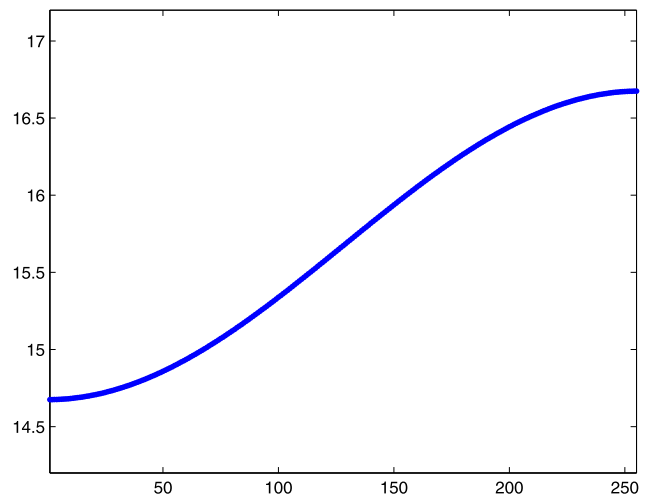


Fig. 1e. Dispersion relation λ_k vs. k . The index k enumerates the frequencies $\lambda_k > 0$ of the continuous spectrum of $J\mathcal{H}$, from smaller to larger. The breather is that of Fig. 1a, computed using $N = 523$ sites.

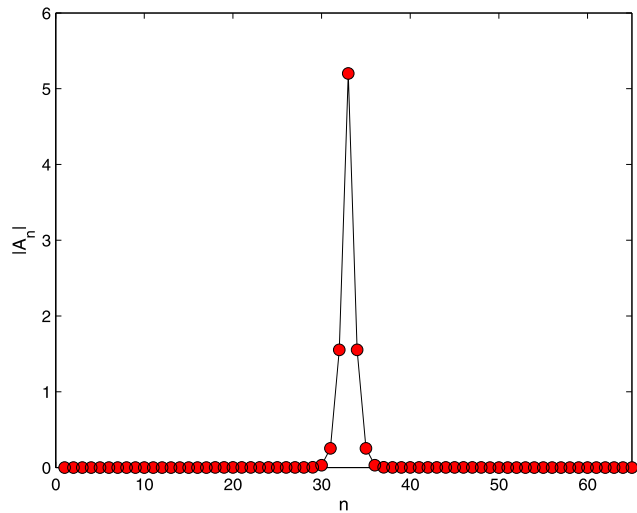


Fig. 2a. $|A_n|$ vs. site number n for a 1-peak breather that is strongly localized at central site $n = 33$. The number of sites is $N = 65$, while $\kappa = 0.25$, $\delta = -0.5$, $\gamma = -1$ (focusing case). The power is $c = 32.0$. The computed frequency is $\omega = 6.97912841$.

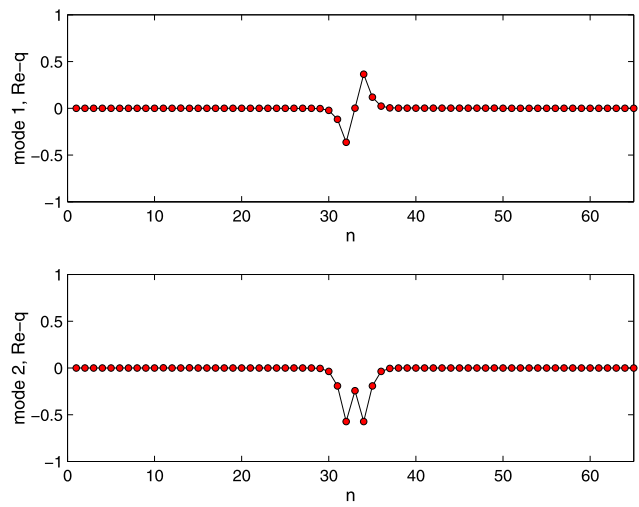


Fig. 2c. q_n vs. n , q -component of real part of eigenvectors of $J\mathcal{H}$ corresponding to eigenvalues $\pm i\lambda_1 = \pm i1.33223569$ (“mode 1”, odd), and $\pm i\lambda_2 = \pm i1.59696824$ (“mode 2”, even) respectively. These are the nonzero eigenvalues that are nearest to the origin.

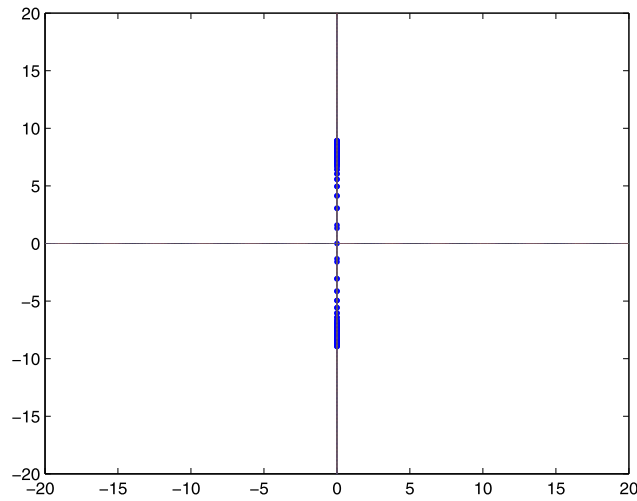


Fig. 2b. Spectrum of $J\mathcal{H}$ around breather of Fig. 2a. Eigenvalues come in pairs $\pm i\lambda$, indicating linear stability. Closer inspection suggests 20 pairs of isolated (point) eigenvalues $\pm i\lambda$, and a remaining set of closely spaced eigenvalues representing continuous spectrum for the infinite problem. The eigenvalues in the continuous band have positive real parts in the interval $[6.98978871, 8.94364354]$.

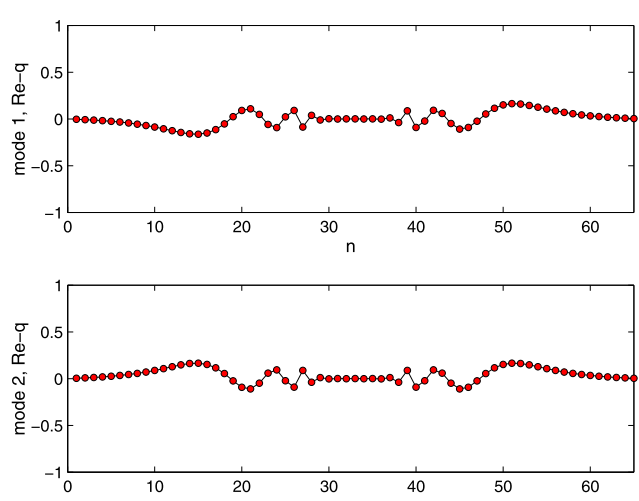


Fig. 2d. q_n vs. n , q -component of real part of eigenvectors of $J\mathcal{H}$ corresponding to eigenvalues $\pm i\lambda_{11} = \pm i6.94179627$ (“mode 19”, odd), and $\pm i\lambda_{12} = \pm i6.94179627$ (“mode 20”, even). These are the highest frequency internal modes.

that varies slightly, and appears to approach $[\omega, \omega + 4\delta]$, e.g. is $[14.675066, 16.6749183]$ for $N = 523$. Thus we believe that first 12 eigenvalues in the positive imaginary axis approximate a point component of the spectrum and represent “internal modes”, while the remaining eigenvalues represent continuous spectrum. In Fig. 2b we indicate a similar situation for a more nonlocal (i.e. smaller κ) breather. The spectrum is closer to the origin, and there is evidence for 20 internal modes.

We also observe that the internal modes may have considerable amplitude away from the peak. Fig. 1c shows the lowest frequency internal modes for the breather of Fig. 1a. Note the maxima at the sites adjacent to the central peak of the breather. By the notation in (3.2) eigenvectors of $J\mathcal{H}$ have q -, and p -components, and are generally complex. Maxima refer to maxima of real or imaginary parts of the q -, or p -components. The internal mode eigenvalues in the positive imaginary axis come in pairs $i\lambda_{2j-1}, i\lambda_{2j} \in i\mathbf{R}$, $j = 1, 2, \dots$, that correspond to one odd and one even eigenvector. The values $\lambda_{2j-1}, \lambda_{2j}$ are too close to see in Fig. 1b, and become closer as j increases. Modes corresponding to λ_j with increasing j generally have maxima that are further from the origin; this is indicated

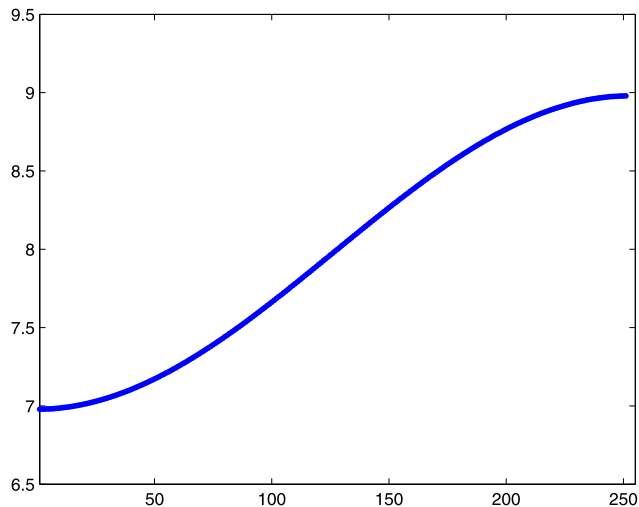


Fig. 2e. Dispersion relation $\text{Im}\lambda_k$ vs. k , where k enumerates the frequencies λ_k in the continuous spectrum of $J\mathcal{H}$, from smaller to larger. The breather is that of Fig. 2a, computed using $N = 523$ sites.

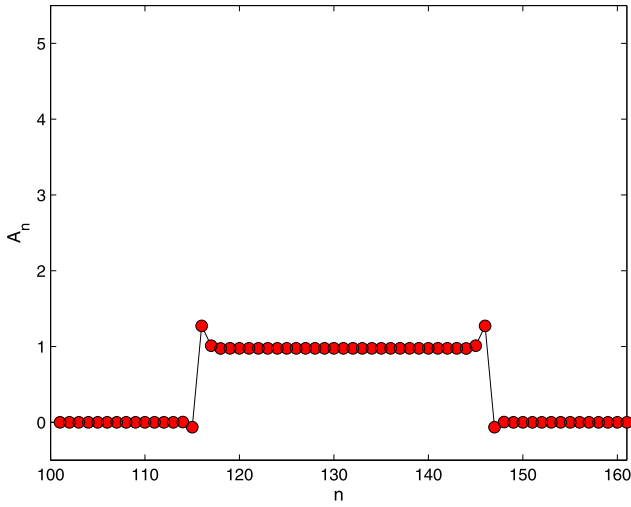


Fig. 3a. A_n vs. site number n for a shelf-like breather. The number of sites is $N = 261$, while $\kappa = 0.8$, $\gamma = -1$, $\delta = 0.05$ (defocusing case). The power is $c = 31.0$.

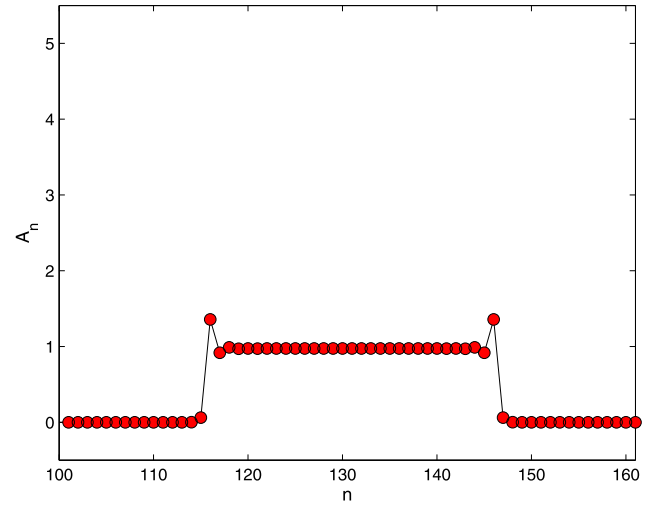


Fig. 4a. A_n vs. site number n for a shelf-like breather. The number of sites is $N = 261$, while $\kappa = 0.8$, $\delta = -0.05$, $\gamma = -1$ (focusing case). The power is $c = 31.0$.

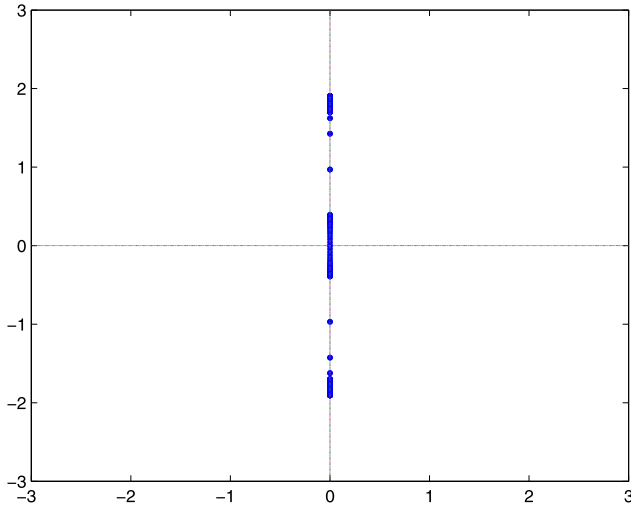


Fig. 3b. Spectrum of $J\mathcal{H}$ around breather of Fig. 3a, indicating linear stability.

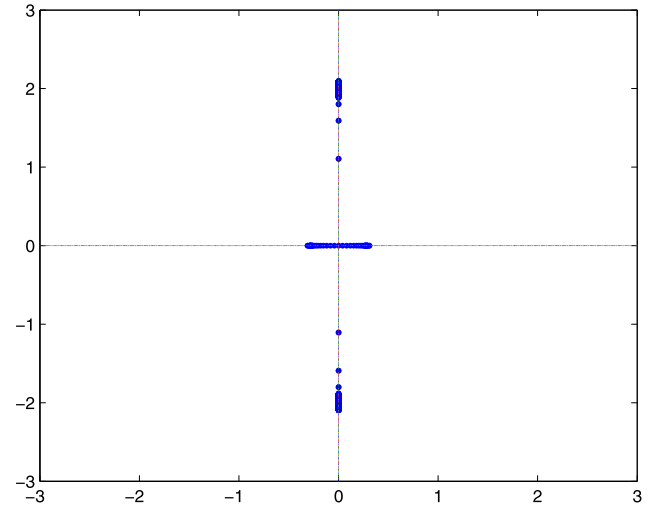


Fig. 4b. Spectrum of $J\mathcal{H}$ around breather of Fig. 4a, indicating linear instability.

in Fig. 1d, where we show the eigenvectors corresponding to the highest frequency internal modes. In Fig. 2d we see that the internal modes extend to about 10–15 sites from the site of the peak.

Figs. 1e, 2e show the continuous band “dispersion” relation for the breathers of Figs. 1, 2 respectively, that is the positive frequencies λ_k of the continuous spectrum versus an index k that enumerates them, from smaller to larger. Note that the corresponding eigenvalues on the positive imaginary axis are double, and we only show one representative from each pair. The shape of the dispersion is similar to that of the free discrete equation $\dot{u} = i\delta\Delta u$, shifted by ω , the frequency of the breather.

The presence of the internal modes may be heuristically understood by examining the one-peak breather solution of the $\delta = 0$ problem. For $\gamma = -1$ this solution has the amplitude $A_0 = A \in \mathbb{R}$, and $A_n = 0, \forall n \in \mathbb{Z} \setminus \{0\}$, and frequency $\omega = 2 \tanh(\kappa/2)A^2$. Also, $A^2 = c$, where c is the power. By (3.5), (3.6), (3.7) the L_+, L_- for this solution reduce to

$$L_+(n, m) = (-\omega + 2 \tanh \frac{\kappa}{2} e^{-\kappa|n|} A^2 + \tanh \frac{\kappa}{2} A^2 \delta_{0,n}) \delta_{n,m}, \quad (3.8)$$

$$L_-(n, m) = (-\omega + 2 \tanh \frac{\kappa}{2} e^{-\kappa|n|} A^2) \delta_{n,m}, \quad (3.9)$$

$n, m \in \mathbb{Z}$. Thus L_+, L_- are diagonal, and $J\mathcal{H}$ is block diagonal with 2×2 blocks $J_2 \mathcal{H}_n, n \in \mathbb{Z}$, with J_2 the 2×2 symplectic matrix, and

\mathcal{H}_n diagonal with $\text{diag}(\mathcal{H}_n) = (L_+(n, n), L_-(n, n))$. By (3.8)

$$\begin{aligned} L_+(n, n) &= L_-(n, n) = \omega(e^{-\kappa|n|} - 1), \quad \forall n \in \mathbb{Z} \setminus \{0\}, \\ L_+(0, 0) &= \tanh \frac{\kappa}{2} A^2, \quad L_-(0, 0) = 0, \end{aligned} \quad (3.10)$$

and we see that the spectrum of $J\mathcal{H}$ consists of a double zero eigenvalue from the block $J\mathcal{H}_0$, and the eigenvalues

$$\pm i\lambda_n, \quad \lambda_n = \omega(1 - e^{-\kappa|n|}), \quad n \in \mathbb{Z} \setminus \{0\}, \quad (3.11)$$

corresponding to the respective blocks $J\mathcal{H}_n, n \in \mathbb{Z} \setminus \{0\}$, i.e. the nonzero eigenvalues start at $\pm i\omega(1 - e^{-\kappa})$, and accumulate to $\pm i\omega$ as $|n|$ increases, at a rate that is slower for smaller κ (stronger nonlocality). Also $J\mathcal{H}_{-n}, J\mathcal{H}_n$ have the same eigenvalues.

The heuristic picture is then that the internal modes observed for $\delta \neq 0$ likely belong to eigenspaces that are continued from the eigenspaces of the $\pm i\lambda_n, \pm i\lambda_{-n}$ eigenvalues corresponding to the smallest $|n|$. The remaining higher $|n|$ subspaces ($|n| \rightarrow \infty$) may not be preserved for $\delta \neq 0$. The continuous spectrum is also likely obtained from the part $-\omega I - \delta\Delta$ of the L_+, L_- , and is not affected by \mathcal{A}, \mathcal{M} .

Figs. 3, 4 show examples of shelf-shaped breathers that are examples of the solutions expected from the continuation for the $\delta = 0$ solutions in Theorem 2.4. The breathers shown correspond to

a configuration with 31 consecutive peaks at the $\delta = 0$ limit. The main feature here is the amplitude peak at the interface, clearly visible for the values $\delta = \pm 0.05$ we use. This effect is seen in more examples, with more general profiles at the sites with nontrivial amplitude at $\delta = 0$. In addition, there is a less pronounced peak at the interface between regions where the nontrivial amplitudes change sign.

Figs. 3b, 4b suggest linear stability and linear instability for the corresponding breathers. There is also evidence for bands, starting at $\pm i\omega$, and of internal modes. Internal modes are also present around multi-peak breathers of the cubic DNLS, but here the number of internal modes is larger than $2 \times k - 2$, k the number of peaks, seen in the cubic DNLS [16].

4. Discussion

We have presented a study of localized solutions of breather type in a discrete NLS with a nonlocal cubic nonlinearity. Our small intersite coupling results show several similarities with the breather solutions of the discrete NLS with power nonlinearity. In the present problem we also have a regime where only the linear coupling is small. In that case the nonlocal nonlinear interaction leads to profiles whose more remarkable feature seems to be the presence of amplitude maxima near interfaces. A question for further work is the classification of real solutions for the regime of small linear coupling. A more general question is the presence of breathers that are not real (modulo a global phase), see [13,16] for the cubic NLS with small linear intersite coupling. Related questions are applicable to other nonlocal periodic media, see e.g. [3,8].

Another interesting effect we report is the apparent presence of internal modes for the one-peak breather. This solution is expected to be a constrained extremum of the Hamiltonian, as in the discrete NLS with cubic power nonlinearity, see [19]. A study of properties of these solutions is currently in progress. A further problem is the analysis of the linearized problem, and the effect of the expected internal modes on the dynamics around the breather. Preliminary numerical work suggests long-lived interactions between the internal modes.

Acknowledgements

We acknowledge helpful discussions with G. Assanto, J.P. Borgna, M. McNeil and D. Rial. L.C., P.P., and A.M. acknowledge par-

tial support by SEP-Conacyt grant 177246, and FENOME. R. Ben acknowledges partial support from grant “Ecuaciones diferenciales dispersivas en aplicaciones tecnológicas”, Misiones al Exterior, Ministerio de la Nación, Republica de Argentina. We also thank the referees for several comments that helped improved the manuscript.

References

- [1] D.S. Bernstein, *Matrix Mathematics*, Princeton University Press, Princeton, 2009.
- [2] C. Conti, M. Peccianti, G. Assanto, Route to nonlocality and observation of accessible solitons, *Phys. Rev. Lett.* 91 (2003) 073901.
- [3] N.K. Efremidis, Nonlocal lattice solitons in the thermal media, *Phys. Rev. A* 77 (2008) 063824.
- [4] A. Fratalocchi, G. Assanto, Discrete light localization in one-dimensional nonlinear lattices with arbitrary nonlocality, *Phys. Rev. E* 72 (2005) 066608.
- [5] A. Fratalocchi, G. Assanto, K.A. Brzdakiewicz, M.A. Karpierz, Discrete propagation and spatial solitons in nematic liquid crystals, *Opt. Lett.* 29 (2004) 1530–1532.
- [6] A. Fratalocchi, G. Assanto, K.A. Brzdakiewicz, M.A. Karpierz, Discrete light propagation and self-trapping in liquid crystals, *Opt. Express* 13 (2005) 1808–1815.
- [7] M. Grillakis, J. Shatah, W. Strauss, Stability theory of solitary waves in the presence of symmetry I, *J. Funct. Anal.* 74 (1987) 160–197.
- [8] Y.K. Kartashov, V.A. Vysloukh, L. Torner, Soliton shape and mobility in optical lattices, *Prog. Opt.* 52 (2009) 63–148.
- [9] R.S. MacKay, S. Aubry, Proof of existence of breathers for time-reversible or Hamiltonian networks of weakly coupled oscillators, *Nonlinearity* 7 (1994) 1623–1643.
- [10] J.M.L. MacNeil, N.F. Smyth, G. Assanto, Exact and approximate solutions for optical solitary waves in nematic liquid crystals, *Physica D* 284 (2014) 1–15.
- [11] P. Panayotaros, Continuation and bifurcation of breathers in a finite discrete NLS equation, *Discrete Contin. Dyn. Syst., Ser. S* 4 (5) (2011) 1227–1245.
- [12] P. Panayotaros, T. Marchant, Solitary waves in nematic liquid crystals, *Physica D* 268 (2014) 106–117.
- [13] P. Panayotaros, D.E. Pelinovsky, Periodic oscillations of discrete NLS solitons in the presence of diffraction management, *Nonlinearity* 21 (2008) 1265–1279.
- [14] M. Peccianti, G. Assanto, Nematicons, *Phys. Rep.* 516 (2012) 147–210.
- [15] M. Peccianti, G. De Luca, G. Assanto, C. Umeton, I.C. Khoo, Electrically assisted self-confinement and waveguiding in planar nematic liquid crystal cells, *Appl. Phys. Lett.* 77 (2000) 7–9.
- [16] D.E. Pelinovsky, P.G. Kevrekidis, D.J. Frantzeskakis, Stability of discrete solitons in nonlinear Schrödinger lattices, *Physica D* 212 (2005) 1–19.
- [17] D. Pelinovsky, A. Sakovich, Internal modes for discrete solitons near the anti-continuum limit of the dNLS equation, *Physica D* 240 (2011) 265–281.
- [18] K.A. Rutkowska, G. Assanto, M.A. Karpierz, Discrete light propagation in arrays of liquid crystalline waveguides, in: G. Assanto (Ed.), *Nematicons: Spatial Optical Solitons in Nematic Liquid Crystals*, Wiley, Hoboken, 2013.
- [19] M.I. Weinstein, Excitation thresholds for nonlinear localized modes on lattices, *Nonlinearity* 12 (1999) 673–691.
- [20] E. Zeidler, *Nonlinear Functional Analysis and Its Applications I*, Springer-Verlag, New York, 1986.